

## Correlated Gene Expression Supports Synchronous Activity in Brain Networks

Jonas Richiardi<sup>1,2,\*†</sup>, Andre Altmann<sup>1,†</sup>, Anna-Clare Milazzo<sup>3,1</sup>, Catie Chang<sup>4</sup>, M. Mallar Chakravarty<sup>5,6</sup>, Tobias Banaschewski<sup>7</sup>, Gareth J. Barker<sup>8</sup>, Arun L.W. Bokde<sup>9</sup>, Uli Bromberg<sup>10</sup>, Christian Büchel<sup>10</sup>, Patricia Conrod<sup>8,11</sup>, Mira Fauth-Bühler<sup>12</sup>, Herta Flor<sup>13</sup>, Vincent Frouin<sup>14</sup>, Jürgen Gallinat<sup>15</sup>, Hugh Garavan<sup>9,16</sup>, Penny Gowland<sup>17</sup>, Andreas Heinz<sup>15</sup>, Hervé Lemaître<sup>18,19</sup>, Karl F. Mann<sup>12</sup>, Jean-Luc Martinot<sup>18,19</sup>, Frauke Nees<sup>13</sup>, Tomáš Paus<sup>20,21</sup>, Zdenka Pausova<sup>22</sup>, Marcella Rietschel<sup>23</sup>, Trevor W. Robbins<sup>24</sup>, Michael N. Smolka<sup>25</sup>, Rainer Spanagel<sup>26</sup>, Andreas Ströhle<sup>15</sup>, Gunter Schumann<sup>8,27</sup>, Mike Hawrylycz<sup>28</sup>, Jean-Baptiste Poline<sup>29</sup>, Michael D. Greicius<sup>1,\*</sup>, and the IMAGEN consortium<sup>‡</sup> (www.imagen-europe.com)

<sup>1</sup>Functional Imaging in Neuropsychiatric Disorders Laboratory, Department of Neurology and Neurological Sciences, Stanford University, Stanford, CA, USA.

<sup>2</sup>Laboratory for neuroimaging and cognition, Department of Neurology and Department of Neurosciences, University of Geneva, Geneva, Switzerland.

<sup>3</sup>Veterans Administration War Related Illness & Injury Study Center, Palo Alto, CA, USA.

<sup>4</sup>Advanced MRI section, National Institutes of Health, Bethesda, MD, USA.

<sup>5</sup>Cerebral Imaging Centre, Douglas Mental Health University Institute, Montreal, Canada

<sup>6</sup>Departments of Psychiatry and Biomedical Engineering, McGill University, Montreal, Canada.

<sup>7</sup>Department of Child and Adolescent Psychiatry, Central Institute of Mental Health, Medical Faculty Mannheim, Heidelberg University, Mannheim, Germany.

<sup>8</sup>Institute of Psychiatry, Psychology and Neuroscience, King's College London, London, United Kingdom.

<sup>9</sup>Institute of Neuroscience, Trinity College Dublin, Dublin, Ireland.

<sup>10</sup>Universitätsklinikum Hamburg Eppendorf, Hamburg, Germany.

<sup>11</sup>Department of Psychiatry, Université de Montréal, CHU Ste Justine Hospital, Montréal, Canada.

<sup>12</sup>Department of Addictive Behaviour and Addiction Medicine, Central Institute of Mental Health, Medical Faculty Mannheim, Heidelberg University, Mannheim, Germany.

<sup>13</sup>Department of Cognitive and Clinical Neuroscience, Central Institute of Mental Health, Medical Faculty Mannheim, Heidelberg University, Mannheim, Germany.

<sup>14</sup>Neurospin, Commissariat à l'Energie Atomique et aux Energies Alternatives, Paris, France.

<sup>15</sup>Department of Psychiatry and Psychotherapy, Campus Charité Mitte, Charité – Universitätsmedizin Berlin, Berlin, Germany.

<sup>16</sup>Departments of Psychiatry and Psychology, University of Vermont, Burlington, VA, USA.

<sup>17</sup>School of Physics and Astronomy, University of Nottingham, United Kingdom.

<sup>18</sup>Institut National de la Santé et de la Recherche Médicale, INSERM Unit 1000 “Neuroimaging & Psychiatry”, University Paris Sud, Orsay, France.

<sup>19</sup>INSERM Unit 1000 at Maison de Solenn, APHP, Cochin Hospital, University Paris Descartes, Sorbonne Paris Cité, Paris, France.

<sup>20</sup>Rotman Research Institute, University of Toronto, Toronto, Canada.

<sup>21</sup>School of Psychology, University of Nottingham, Nottingham, United Kingdom.

<sup>22</sup>The Hospital for Sick Children, University of Toronto, Toronto, Canada.

<sup>23</sup>Department of Genetic Epidemiology in Psychiatry, Central Institute of Mental Health, Medical Faculty Mannheim, Heidelberg University, Mannheim, Germany.

<sup>24</sup>Behavioural and Clinical Neuroscience Institute and Department of Psychology, University of Cambridge, Cambridge, United Kingdom.

<sup>25</sup>Department of Psychiatry and Psychotherapy, and Neuroimaging Center, Technische Universität Dresden, Dresden, Germany.

<sup>26</sup>Department of Psychopharmacology, Central Institute of Mental Health, Faculty of Clinical Medicine Mannheim

<sup>27</sup>MRC Social, Genetic and Developmental Psychiatry (SGDP) Centre, London, United Kingdom.

<sup>28</sup>Allen Institute for Brain Science, Seattle, WA, USA.

<sup>29</sup>Helen Wills Neuroscience Institute, University of California Berkeley, Berkeley, CA, USA.

\*Correspondence to: [jonas.richiardi@unige.ch](mailto:jonas.richiardi@unige.ch), [greicius@stanford.edu](mailto:greicius@stanford.edu)

†These authors contributed equally

‡IMAGEN consortium authors and affiliations are listed in the supplementary materials

During rest, brain activity is synchronized between different regions widely distributed throughout the brain, forming functional networks. However, the molecular mechanisms supporting functional connectivity remain undefined. We show that functional brain networks defined with resting-state fMRI can be recapitulated using measures of correlated gene expression in a post-mortem brain tissue dataset. The set of 136 genes we identify is significantly enriched for ion channels. Polymorphisms in this set of genes significantly impact resting-state functional connectivity in a large sample of healthy adolescents. Expression levels of these genes are also significantly associated with axonal connectivity in the mouse. The results provide convergent, multimodal evidence that resting-state functional networks correlate with the orchestrated activity of dozens of genes linked to ion channel activity and synaptic function.

Functional brain networks, as detected by resting-state fMRI, are linked to the correlated expression of dozens of neurotransmitter and ion channel-related genes.

Brain activity at rest exhibits intrinsic low-frequency synchronization between anatomically distinct brain regions(1). When observed with functional magnetic resonance imaging (fMRI), this coherence between regions (*functional connectivity*) defines 15-20 brain networks associated with such canonical functions such as vision, language, episodic memory, and spatial attention(2-4). These functional networks are disrupted in several neurodegenerative and neuropsychiatric diseases(5), and may constitute the maps followed by neurodegenerative diseases marching, trans-synaptically across the brain(6). While it has been shown that connectivity within the default-mode network (DMN)(7) and topological measures of whole-

brain networks(8) are heritable, the set of genes promoting functional connectivity remains unknown. To pursue this question, we applied a network modeling approach to both neuroimaging and gene expression data.

Using resting-state fMRI data from 15 healthy right-handed subjects (8 females, age range 18-29), we computed 14 well-known and reproducible functional networks(9) (Fig. S1) by using independent component analysis (ICA). We then mapped samples from the Allen Institute for Brain Science (AIBS) human microarray dataset(10) (six subjects, two contributed both hemispheres, four contributed one hemisphere, one female, age range 24-57, totaling 3,702 brain samples; Table S1) to these networks by using normalized Montreal Neurological Institute (MNI) coordinates. To avoid biases due to gross transcriptional dissimilarities in different brain regions, we excluded basal ganglia, cerebellum, and deep gray matter (including hippocampus), leaving only cortex samples (Data File S1). This removed the basal ganglia network, leaving 13 networks. Of 1777 cortex samples, 501 were mapped to the 13 functional networks, and 1276 to “non-network” regions of the brain. We focused the analysis on four large non-overlapping networks: dorsal default-mode (dDMN), salience, sensorimotor, and visuospatial (Fig. 1A), comprising 241 samples total. These four networks were chosen because they are well-characterized in the imaging literature (2, 11–14), consist of non-contiguous regions in both hemispheres, and have adequate coverage in the AIBS data (Fig. 1B).

[Figure 1 here]

**Fig. 1 Functional networks in MRI and gene expression data.**

*A* The four functional networks of interest. red: dorsal default-mode, yellow: salience, green: visuospatial, blue: sensorimotor. *B* AIBS brain samples assigned to their corresponding functional network. Full circles are samples assigned to the four networks of interest, empty circles show samples in the 9 other networks, dots show non-network AIBS samples

We used the transcriptional similarity of gene expression profiles between brain tissue samples to define *correlated gene expression networks*. In mouse brains, transcriptional similarity reflects cytoarchitecture(15), but in human brains the differences are more subtle across the neocortex(10). As opposed to gene co-expression networks, which quantify gene-gene relationship across tissue samples(16), a correlated gene expression network quantifies tissue-tissue relationships across genes. Nodes were defined by brain tissue samples (Fig. 1B); edges were weighted by similarity between vectors of gene expression values at each sample. After preprocessing and assigning one probe for each of the 16,906 genes(17) (Data File S2), we measured expression similarity by Pearson correlation(17), setting negative correlations to zero. Then we asked whether there are observable genetic correlates for the functional network organization: are gene expression correlations in functionally grouped regions higher than can be expected by chance?

We defined the strength fraction in functional networks as a measure of the relationship between correlated gene expression within and outside the set of functional networks of interest. Denoting  $W$  the sum of all edge weights within all functional networks,  $W_i$  the sum of weights

within the 4 functional networks of interest, and T the brain graph's total strength (sum of all edge weights linking the full 1777-nodes graph), the strength fraction is  $S=W_i/(T-W)$ . Higher values of S mean the samples in the set of functional networks are more similar to each other, relative to the remaining brain regions (Fig. S2). Significance was assessed using permutation testing(18), randomly reshuffling 10,000 times the sample-to-network assignment in the full 1777-nodes graph. In addition to considering only cortex samples, to avoid biasing results towards similar tissues(10), before computation, we removed edges linking two samples belonging to the same tissue class (defined by regional ontology: Fig. S3, Table S4). Grouping gene expression samples according to functional networks yielded a higher strength fraction than other groupings of samples: the spatial organization of functional networks corresponded to regions that have more highly correlated gene expression than expected by chance ( $p < 10^{-4}$ ). Given that we used only cortical samples, that we removed edges linking tissues of the same class, and that functional networks are spatially distributed, this finding cannot emerge from spatial proximity or gross tissue similarity.

We next sought to identify which genes, specifically, drive the relationship between correlated gene expression and functional networks. We computed the marginal influence of each gene on strength fraction of all four functional networks together(17), and ranked genes across all six different two-way splits of the six subjects(17). Then, we computed list overlap statistics(19) between the two brain subgroups at a false discovery rate (FDR) of 5%. Combining results from six splits, the final list was obtained via stability selection(20), selecting genes that appear in the majority of splits (four or more out of six). This resulted in a consensus list of 136 genes (Table S2).

We validated our findings in vivo (supplementary online text), using paired genome-wide single nucleotide polymorphism (SNP) data and resting state fMRI (rs-fMRI) recordings in  $N = 259$  14 year olds (126 females) from the IMAGEN database(21), which has more subjects but not all were usable(17) (Data File S3). The strength fraction for the combined four networks in the rs-fMRI data was computed for every subject (as in the AIBS gene expression data), and used as a quantitative imaging phenotype in a genome-wide association study (GWAS)(Fig. S4), correcting for several covariates including motion. We computed a Z-statistic(22) for the enrichment of p-values in the consensus list. Genetic variation in the consensus list was significantly associated with in-vivo rs-fMRI strength fraction ( $Z = 2.55$ ,  $p = 0.006$ ). Thus, not only gene expression levels but also common polymorphisms in the consensus genes were related to the strength of functional networks. Subjects at both ends of the spectrum of multilocus genetic scores (representing the multiallelic effect of the genes in the consensus list on the functional connectivity phenotype(17)) showed definite differences in functional connectivity strength mostly within the functional networks themselves, but also between the functional networks (Figs. 2, S5).

[Figure 2 here]

**Fig. 2: In-vivo functional connectivity differences related to the consensus gene list.**

*Difference in in-vivo functional connectivity between the averages of the top 20 and the bottom 20 subjects in IMAGEN, ranked by genotype score with respect to the consensus list of genes. **A** Difference matrix sorted by functional network (correlation differences smaller than  $|0.05|$  not shown). Positive values indicate connections that are stronger in high genotype score subjects, negative values the opposite. Connections are mostly increased within functional networks, but also between some functional networks. **B** MNI space sagittal view of within-network connections that are stronger in high genotype score subjects. Regions (disks) are coded according to the functional network they belong to: red: dorsal default-mode, yellow: salience, green: visuospatial, blue: sensorimotor. Connections (lines) are color-coded to their functional networks. **C** Same, for connections that are stronger in low genotype score subjects. The majority of connections are strengthened in high genotype score subjects.*

We next investigated the relationship between our gene list and the connectivity of axonal projections underlying functional networks. We used the Allen Institute mouse brain atlas (15), which offers finely sampled whole-genome expression data, together with a recent meso-scale model of mouse connectivity derived from the Allen Mouse Brain Connectivity Atlas (AMBCA) (23). To match human data, we focused on the mouse isocortex, and used a 38-region parcellation (23) (Fig. 3A). With 57 mouse orthologs for our consensus gene list, we obtained a correlated gene expression network, representing transcriptional similarity between these 38 regions. We computed a normalized, symmetric connectivity matrix from the significant connections in the ipsilateral connectivity model of the AMBCA(17). We tested the association

between mouse connectivity graph and transcriptional similarity graph (Figs. 3B, 3C) using a modified Mantel procedure, whereby we randomly selected gene subsets of the same size as our ortholog consensus list 10,000 times to obtain a null distribution. The correlation between transcriptional similarity in these 38 meso-scale isocortex regions and their axonal connectivity was significantly higher when using our list than expected by chance ( $p = 0.011$ , or  $p = 0.022$  when using the contralateral connectivity model).

[Figure 3 here]

**Fig. 3: Mouse meso-scale connectivity and transcriptional similarity.**

*A* Mouse isocortex parcellated into 38 regions (23); *B* corresponding symmetrized, thresholded, and normalized ipsilateral axonal connectivity weights; *C* transcriptional similarity (genetic correlation) using our consensus list of genes.

Finally, we categorized the consensus gene list using Gene Ontology (GO), by computing statistical overrepresentation for Biological Processes (BP), Cellular Component (CC), and Molecular Function (MF) with the Database for annotation, visualization and integrated discovery (DAVID) 6.7(24). The only significant MF annotation ( $p < 0.05$ , Benjamini-Hochberg False Discovery Rate ( $FDR_{BH}$ )-corrected) related to ion transport. No BP annotation was significant. Four out of six significant CC annotations ( $p < 0.03$   $FDR_{BH}$ ) concerned ion channels, in particular involving sodium channels such as SCN4B or receptors such as GABRA5 (Full annotation list: Tables S5, S6). Significant associations with 9 diseases, including Alzheimer's disease and schizophrenia ( $p < 0.05$   $FDR_{BH}$ ), which are network disorders, were also found

(Table S10). We validated annotations in-vivo on IMAGEN data, by restricting the analysis to these 7 significant GO terms. Genetic variation in all but 1 GO term was significantly associated with in vivo functional connectivity ( $Z > 4.02$ ,  $p < 2.8 \times 10^{-5}$  uncorrected; Table S9). Using a mouse transcriptome database(25), we also found that 39 mouse orthologs from our list were significantly enriched in neurons, 19 in astrocytes, and 14 in oligodendrocytes (76 were not significantly overexpressed in any of these 3 cell types). This suggests that the relationship between gene expression and spatial organization into functional networks may be due to neuronal processes more than to support cell or white matter processes.

Functional networks are fundamental to many brain processes in humans. Here we showed that network strength was correlated with the expression of genes tightly linked to synaptic function. The preservation of the association between functional networks and gene expression across the lifespan (IMAGEN: 14 year olds, AIBS: 24-55) is remarkable, and could be partly explained by the relative stabilization of inter-regional transcriptional similarity from adolescence onwards(26). Genes in our list may also play a role in certain diseases: some are implicated in brain disorders like Alzheimer and schizophrenia(27) whose pathogenesis is thought to relate, in part, to aberrant connectivity. Beyond humans, it appears that similar mechanisms extend to lower animals, because our list is significantly associated with mouse neural connectivity, and several gene functions from our list were found in a study examining genes supporting neural connectivity in rodents(28) (Tables S3, S7, S8). Thus, our results show that across developmental stages and species, functional connectivity in brain networks is integrally linked to the machinery of synaptic communication.

## References and Notes:

1. M. D. Fox, M. E. Raichle, Spontaneous fluctuations in brain activity observed with functional magnetic resonance imaging. *Nat Rev Neurosci.* **8**, 700–711 (2007).
2. S. M. Smith *et al.*, Correspondence of the brain's functional architecture during activation and rest. *Proc. Natl. Acad. Sci.* **106**, 13040–13045 (2009).
3. R. M. Birn, The role of physiological noise in resting-state functional connectivity. *Neuroimage.* **62**, 864–870 (2012).
4. Z. Shehzad *et al.*, The resting brain: unconstrained yet reliable. *Cereb. Cortex.* **19**, 2209–2229 (2009).
5. M. D. Fox, M. Greicius, Clinical applications of resting state functional connectivity. *Front Syst Neurosci.* **4**, 19 (2010).
6. W. W. Seeley, R. K. Crawford, J. Zhou, B. L. Miller, M. D. Greicius, Neurodegenerative Diseases Target Large-Scale Human Brain Networks. *Neuron.* **62**, 42–52 (2009).
7. D. C. Glahn *et al.*, Genetic control over the resting brain. *Proc Natl Acad Sci US A.* **107**, 1223–1228 (2010).
8. A. Fornito *et al.*, Genetic influences on cost-efficient organization of human cortical functional networks. *J Neurosci.* **31**, 3261–3270 (2011).
9. W. R. Shirer, S. Ryali, E. Rykhlevskaia, V. Menon, M. D. Greicius, Decoding Subject-Driven Cognitive States with Whole-Brain Connectivity Patterns. *Cereb. Cortex.* **22**, 158–165 (2012).
10. M. J. Hawrylycz *et al.*, An anatomically comprehensive atlas of the adult human brain transcriptome. *Nature.* **489**, 391–399 (2012).
11. D. Mantini, M. G. Perrucci, C. Del Gratta, G. L. Romani, M. Corbetta, Electrophysiological signatures of resting state networks in the human brain. *Proc Natl. Acad. Sci. USA.* **104**, 13170–13175 (2007).
12. N. U. F. Dosenbach *et al.*, Distinct brain networks for adaptive and stable task control in humans. *Proc. Natl. Acad. Sci.* **104**, 11073–11078 (2007).
13. Y. Golland, P. Golland, S. Bentin, R. Malach, Data-driven clustering reveals a fundamental subdivision of the human cortex into two global systems. *Neuropsychologia.* **46**, 540–553 (2008).
14. S. D. Roosendaal *et al.*, Resting state networks change in clinically isolated syndrome. *Brain.* **133**, 1612–1621 (2010).
15. L. Ng *et al.*, An anatomic gene expression atlas of the adult mouse brain. *Nat Neurosci.* **12**, 356–362 (2009).
16. B. Zhang, S. Horvath, A general framework for weighted gene co-expression network analysis. *Stat. Appl. Genet. Mol. Biol.* **4**, Article17 (2005).
17. Materials and methods are available as supplementary material on Science Online.

18. J. Richiardi, A. Altmann, M. Greicius, in *Proc. 3rd International Workshop on Pattern Recognition in NeuroImaging (PRNI)* (Philadelphia, USA, 2013), pp. 70–73.
19. L. Natarajan, M. Pu, K. Messer, Statistical tests for the intersection of independent lists of genes: Sensitivity, FDR, and type I error control. *Ann. Appl. Stat.* **6**, 521–541 (2012).
20. N. Meinshausen, P. Buehlmann, Stability selection. *J. R. Stat. Soc. Ser. B (Statistical Methodol.* **72**, 417–473 (2010).
21. G. Schumann *et al.*, The IMAGEN study: reinforcement-related behaviour in normal brain function and psychopathology. *Mol Psychiatry.* **15**, 1128–1139 (2010).
22. D. Nam, J. Kim, S.-Y. Kim, S. Kim, GSA-SNP: a general approach for gene set analysis of polymorphisms. *Nucleic Acids Res.* **38**, W749–W754 (2010).
23. S. W. Oh *et al.*, A mesoscale connectome of the mouse brain. *Nature.* **508**, 207–214 (2014).
24. D. W. Huang, B. T. Sherman, R. A. Lempicki, Systematic and integrative analysis of large gene lists using DAVID bioinformatics resources. *Nat Protoc.* **4**, 44–57 (2008).
25. J. D. Cahoy *et al.*, A transcriptome database for astrocytes, neurons, and oligodendrocytes: a new resource for understanding brain development and function. *J Neurosci.* **28**, 264–278 (2008).
26. M. Pletikos *et al.*, Temporal Specification and Bilaterality of Human Neocortical Topographic Gene Expression. *Neuron.* **81**, 321–332 (2014).
27. A. Heck *et al.*, Converging Genetic and Functional Brain Imaging Evidence Links Neuronal Excitability to Working Memory, Psychiatric Disease, and Brain Activity. *Neuron* (2014), doi:10.1016/j.neuron.2014.01.010.
28. L. Wolf, C. Goldberg, N. Manor, R. Sharan, E. Ruppin, Gene expression in the rodent brain is associated with its regional connectivity. *PLoS Comput Biol.* **7**, e1002040 (2011).
29. C. Chang, G. H. Glover, Effects of model-based physiological noise correction on default mode network anti-correlations and correlations. *Neuroimage.* **47**, 1448–1459 (2009).
30. M. D. Greicius, G. Srivastava, A. L. Reiss, V. Menon, Default-mode network activity distinguishes Alzheimer’s disease from healthy aging: Evidence from functional MRI. *Proc. Natl. Acad. Sci.* **101**, 4637–4642 (2004).
31. K. R. A. Van Dijk *et al.*, Intrinsic Functional Connectivity As a Tool For Human Connectomics: Theory, Properties, and Optimization. *J. Neurophysiol.* **103**, 297–321 (2010).
32. V. Michel *et al.*, A Supervised Clustering Approach for fMRI-based Inference of Brain States. *Pattern Recognit.* **45**, 2041–2049 (2012).
33. Allen Institute for Brain Science, “Case qualification and donor profiles” (2013).
34. Allen Institute for Brain Science, “Microarray data normalization” (2013).
35. W. J. Kent *et al.*, The human genome browser at UCSC. *Genome Res.* **12**, 996–1006 (2002).

36. A. Zalesky, A. Fornito, E. Bullmore, On the use of correlation as a measure of network connectivity. *Neuroimage*. **60**, 2096–2106 (2012).
37. J. Yang, J. Leskovec, in *Proceedings of the ACM SIGKDD Workshop on Mining Data Semantics* (2012), p. 3.
38. D. A. Hosack, G. Dennis Jr, B. T. Sherman, H. C. Lane, R. A. Lempicki, Identifying biological themes within lists of genes with EASE. *Genome Biol.* **4**, R70 (2003).
39. Y. Benjamini, Y. Hochberg, Controlling the False Discovery Rate: A Practical and Powerful Approach to Multiple Testing. *J. R. Stat. Soc. Ser. B.* **57**, 289–300 (1995).
40. H. Mi, A. Muruganujan, P. D. Thomas, PANTHER in 2013: modeling the evolution of gene function, and other gene attributes, in the context of phylogenetic trees. *Nucleic Acids Res.* **41**, D377–D386 (2013).
41. T. A. Eyre, M. W. Wright, M. J. Lush, E. A. Bruford, {HCOP}: a searchable database of human orthology predictions. *Br. Bioinform.* **8**, 2–5 (2007).
42. M. Jenkinson, C. F. Beckmann, T. E. J. Behrens, M. W. Woolrich, S. M. Smith, FSL. *Neuroimage*. **62**, 782–790 (2012).
43. M. Jenkinson, P. Bannister, M. Brady, S. Smith, Improved optimization for the robust and accurate linear registration and motion correction of brain images. *Neuroimage*. **17**, 825–841 (2002).
44. S. Purcell *et al.*, PLINK: A Tool Set for Whole-Genome Association and Population-Based Linkage Analyses. *Am. J. Hum. Genet.* **81**, 559–575 (2007).
45. K. R. A. Van Dijk, M. R. Sabuncu, R. L. Buckner, The influence of head motion on intrinsic functional connectivity MRI. *Neuroimage*. **59**, 431–438 (2012).
46. J. D. Power *et al.*, Methods to detect, characterize, and remove motion artifact in resting state {fMRI}. *Neuroimage*. **84**, 320–341 (2014).
47. J. Yang, S. H. Lee, M. E. Goddard, P. M. Visscher, GCTA: A Tool for Genome-wide Complex Trait Analysis. *Am. J. Hum. Genet.* **88**, 76–82 (2011).
48. K. Wang, M. Li, H. Hakonarson, Analysing biological pathways in genome-wide association studies. *Nat Rev Genet.* **11**, 843–854 (2010).
49. S.-Y. Kim, D. J. Volsky, PAGE: parametric analysis of gene set enrichment. *BMC Bioinformatics.* **6**, 144 (2005).
50. K. Wang, M. Li, M. Bucan, Pathway-based approaches for analysis of genomewide association studies. *Am J Hum Genet.* **81**, 1278–1283 (2007).
51. E. S. Lein *et al.*, Genome-wide atlas of gene expression in the adult mouse brain. *Nature.* **445**, 168–176 (2007).
52. A. Y. Ng, M. I. Jordan, Y. Weiss, On spectral clustering: Analysis and an algorithm. *Adv. Neural Inf. Process. Syst.* **2**, 849–856 (2002).

53. F. Abdelnour, H. U. Voss, A. Raj, Network diffusion accurately models the relationship between structural and functional brain connectivity networks. *Neuroimage*. **90**, 335–347 (2014).
54. M. Meila, J. Shi, in *Proc. Int. Conf. on Artificial Intelligence and Statistics (AISTATS)* (Key West, Florida, USA, 2001).
55. N. Mantel, The Detection of Disease Clustering and a Generalized Regression Approach. *Cancer Res.* (1967).

### **Acknowledgments:**

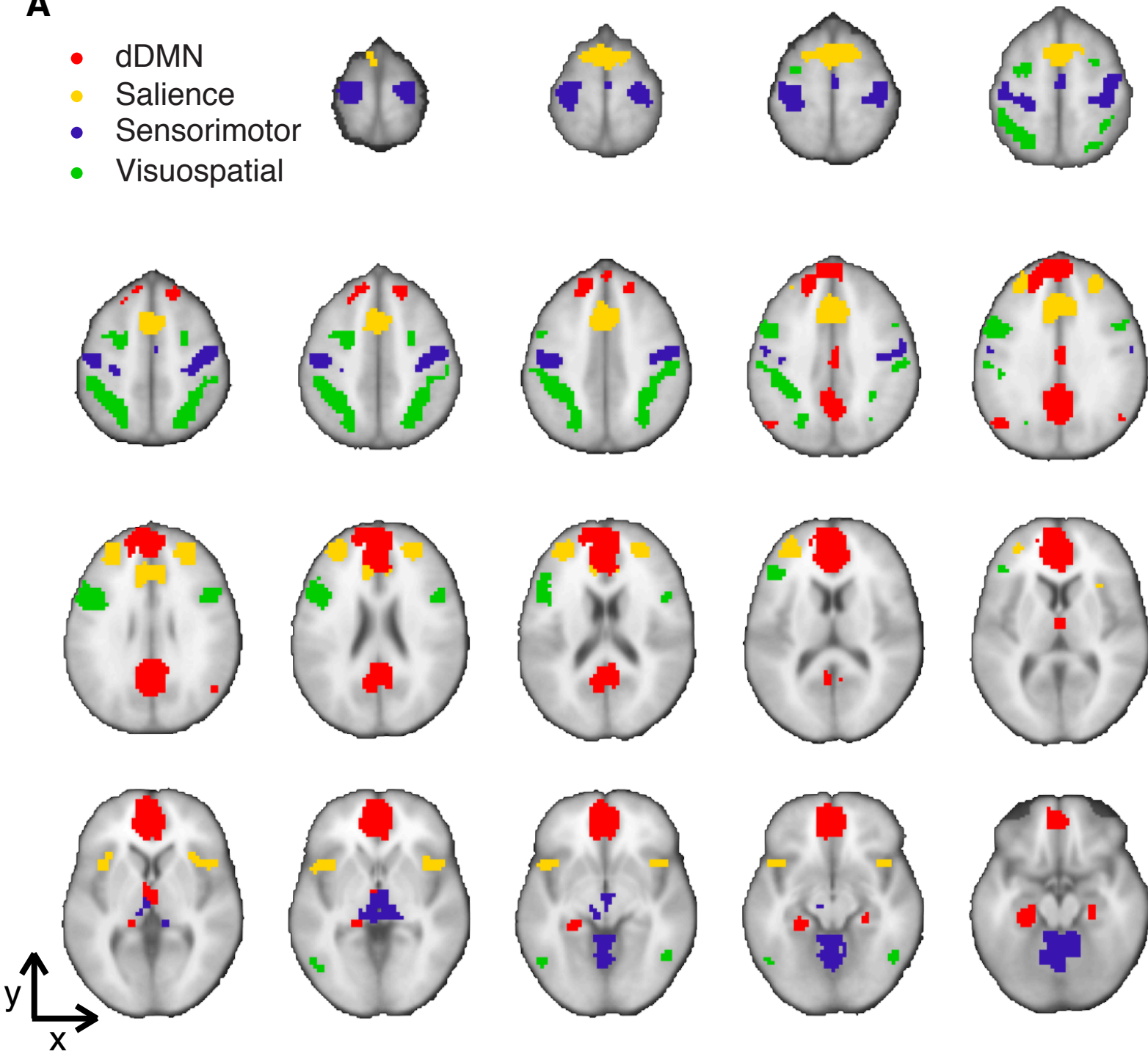
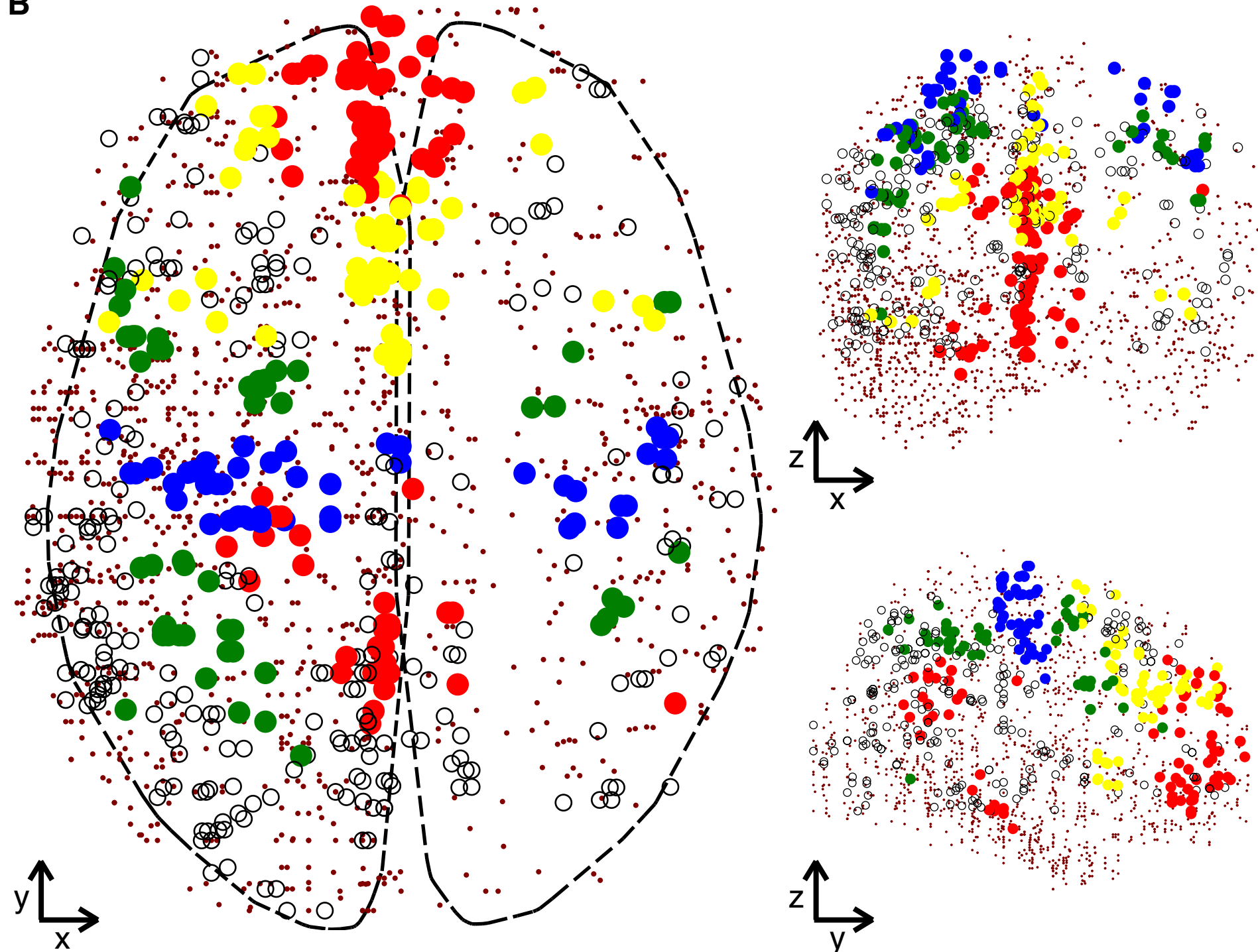
We thank C-K Lee for help with AIBS data normalization, C. Quairiaux for help with mouse brain anatomy.

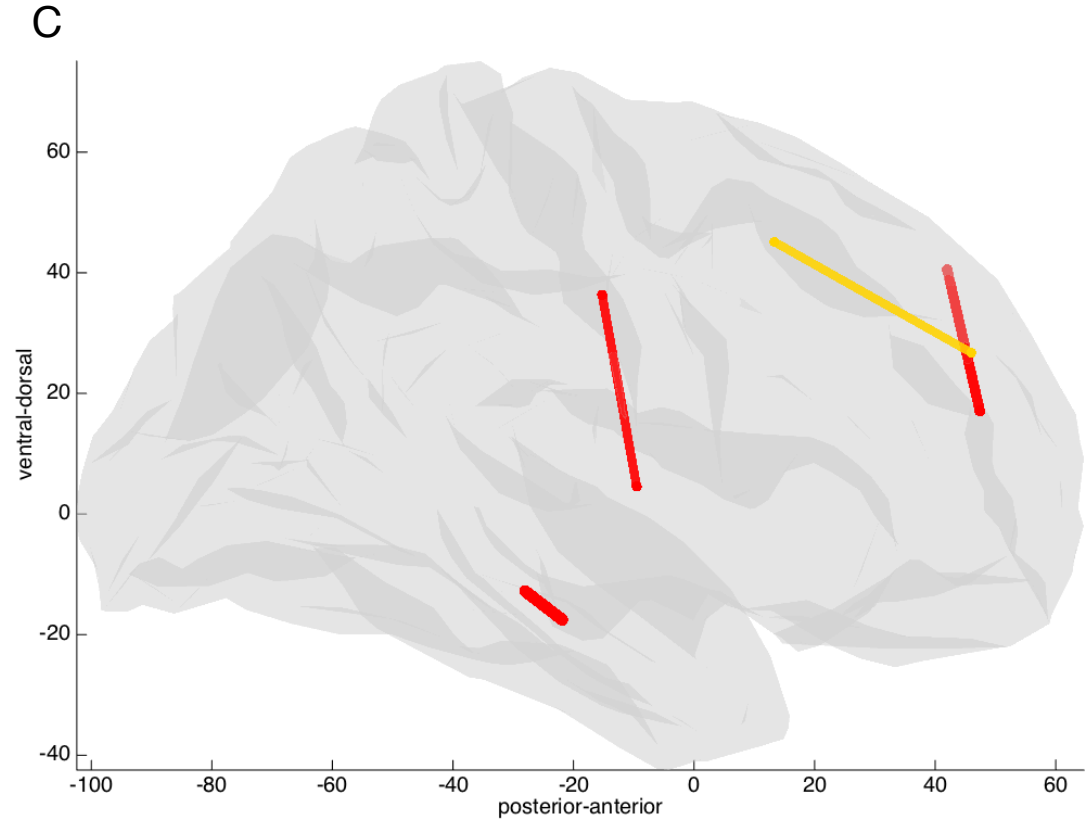
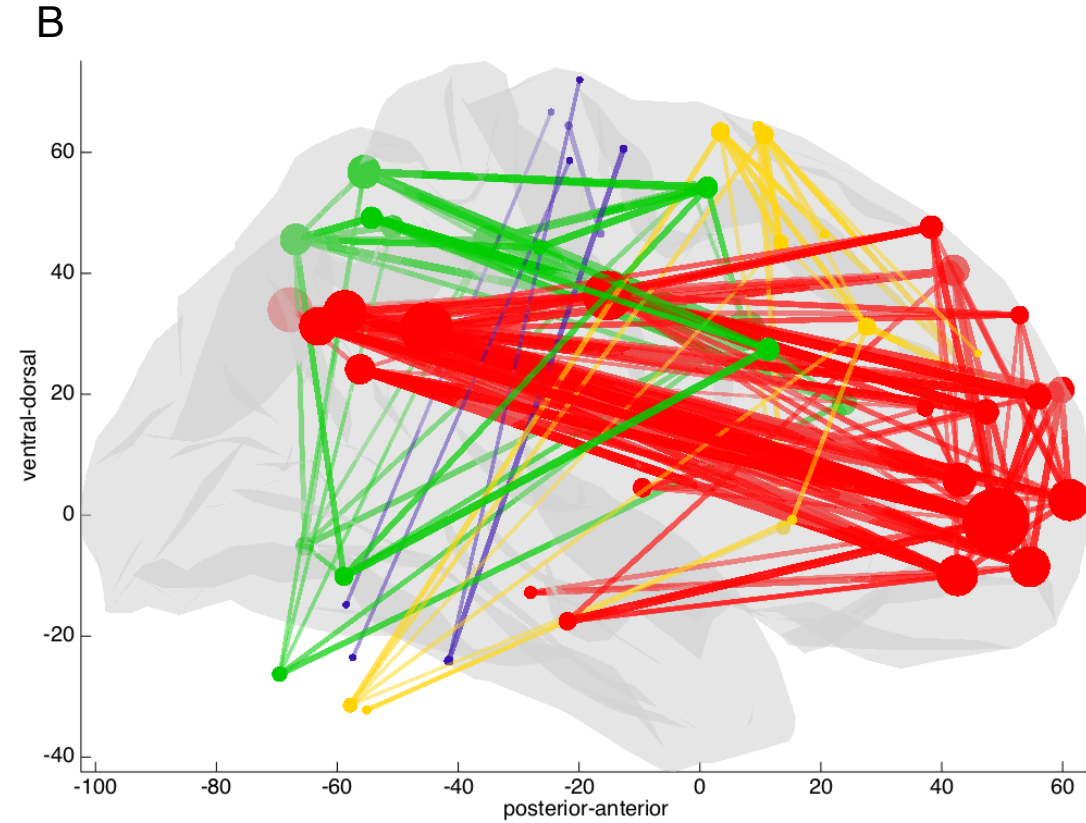
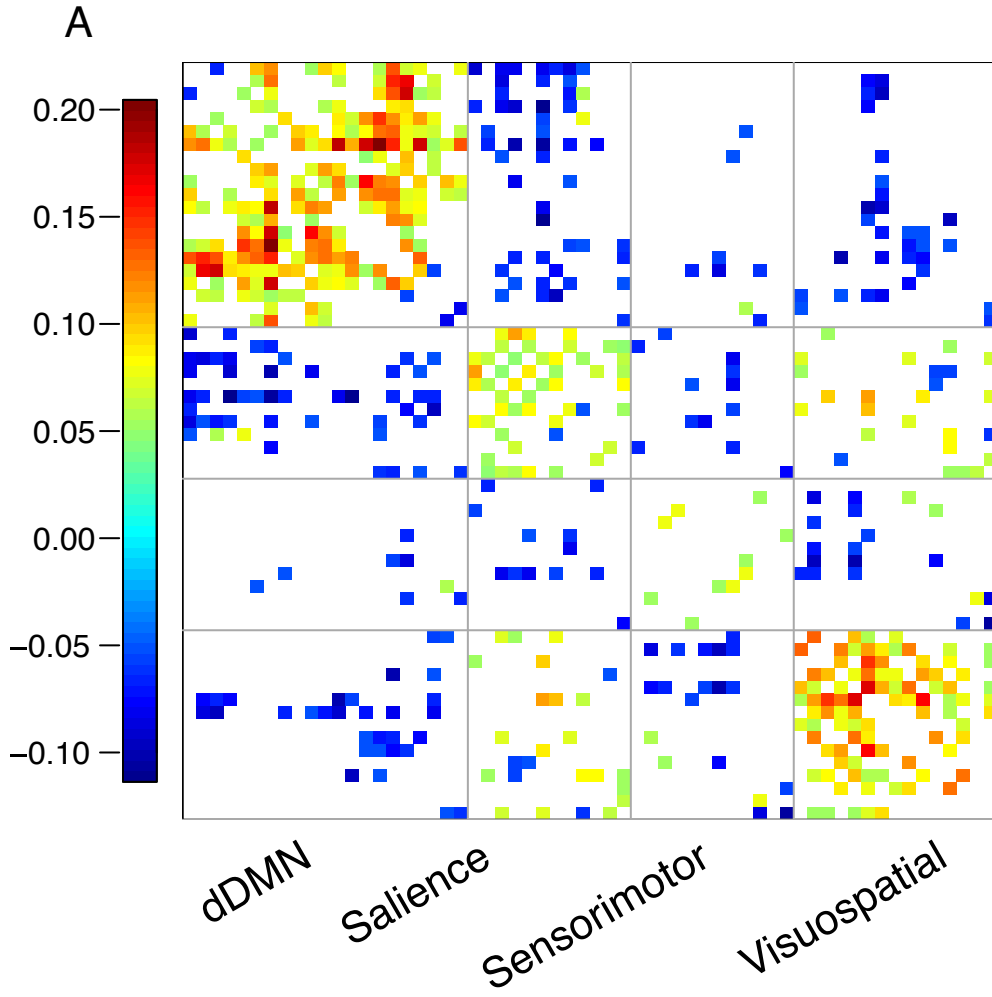
Functional networks imaging data is at [http://findlab.stanford.edu/functional\\_ROIs.html](http://findlab.stanford.edu/functional_ROIs.html). Human microarray data is at <http://human.brain-map.org/>. IMAGEN data is available by application to consortium co-ordinator Prof. Schumann (<http://imagen-europe.com/>), following evaluation according to an established procedure. Mouse gene expression data is at <http://mouse.brain-map.org>. Connectivity model data is from(23).

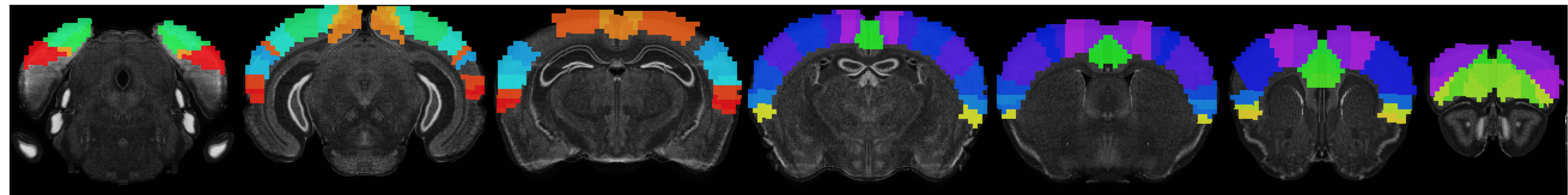
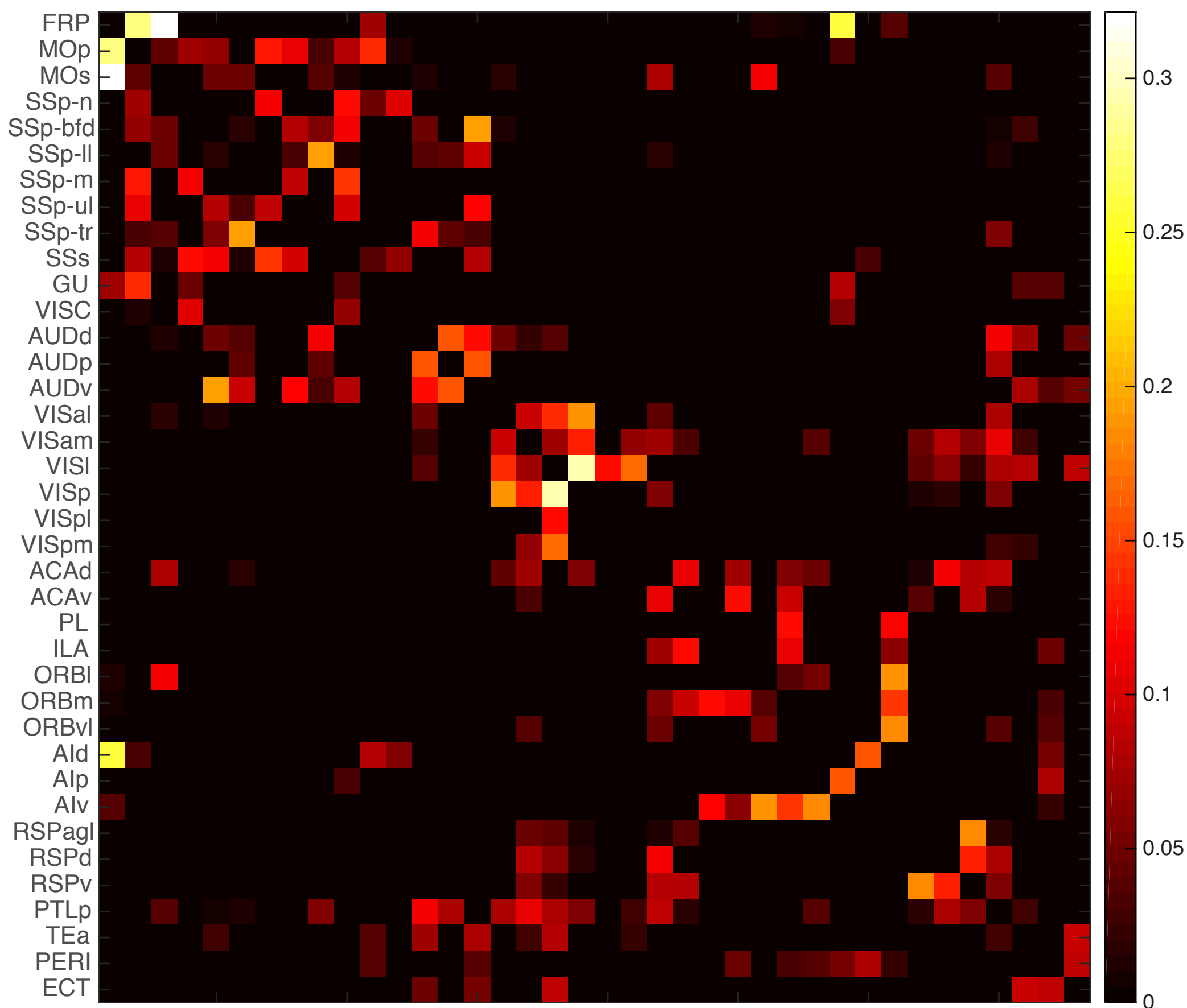
JR is supported by a Marie Curie Fellowship from the European Union (299500). MG is supported by grants from the Feldman Family Foundation and the National Institutes of Health (RO1NS073498). This work received additional support from the following sources: the European Union-funded FP6 Integrated Project IMAGEN (Reinforcement-related behaviour in normal brain function and psychopathology) (LSHM-CT- 2007-037286), the FP7 projects IMAGEMEND(602450; IMAGING GENetics for MENTAL Disorders) and MATRICS (603016), the Innovative Medicine Initiative Project EU-AIMS (115300-2), a Medical Research Council Programme Grant “Developmental pathways into adolescent substance abuse” (93558), the Swedish funding agency FORMAS, the Medical Research Council and the Wellcome Trust (Behavioural and Clinical Neuroscience Institute, University of Cambridge), the National Institute for Health Research (NIHR) Biomedical Research Centre at South London and Maudsley NHS Foundation Trust and King’s College London, the Bundesministerium für Bildung und Forschung (BMBF grants 01GS08152; 01EV0711; eMED SysAlc01ZX1311A; Forschungsnetz AERIAL), the Deutsche Forschungsgemeinschaft (DFG grants SM 80/7-1, SM 80/7-2, SFB 940/1)the National Institutes of Health, U.S.A. (Axon, Testosterone and Mental Health during Adolescence; RO1 MH085772-01A1), by NIH Consortium grant U54 EB020403, supported by a cross-NIH alliance that funds Big Data to Knowledge Centers of Excellence.

**A**

- dDMN
- Saliency
- Sensorimotor
- Visuospatial

**B**



**A****B****C**